

Fig. 2. Cross-sectional TEM image of the MBG (on the right) and electron diffraction from the Al/Zr multilayer stack (on the left).

relief of the substrate and the geometry of magnetron deposition. The sawtooth substrate caused a shadowing for part of the impinging atom flux which arrived at the substrate from different directions and angles because of the large dimensions of the magnetron source. Despite these factors the Al/Zr multilayer demonstrates a remarkable smoothing ability which dominates over shadowing effects and results in suppression of the columnar growth regime.

The Al/Zr multilayer consists of polycrystalline layers of Al and Zr with some amorphous interfaces. While smoothing has usually been observed for amorphous materials or multilayers composed of at least one amorphous layer [9], the Al/Zr example shows that polycrystalline materials also can provide effective smoothing of sawtooth substrates. At the same time intrinsic roughness of crystalline layers, which is caused by a size and shape of crystal grains, is expected to be higher compared to amorphous/amorphous or amorphous/crystalline multilayers. Indeed, the surface roughness of 0.27 nm rms was measured for the flat Al/Zr witness over a $1 \times 1 \mu\text{m}^2$ area, while the same measurements yielded roughness of 0.15 nm rms for a flat Mo/Si multilayer. Although the Al/Zr roughness is tolerable for EUV wavelengths, such a roughening/smoothing behavior is not optimal for sawtooth substrates. An ideal multilayer should provide effective smoothing in the high-frequency range in order to relax surface height variations caused by the stochastic nature of the deposition process, and at the same time minimize smoothing in the medium frequency range in order to provide replication of the groove profile with minimal changes.

Amorphous layers as thick as 1.5 nm are formed at the Al/Zr interfaces via bulk interdiffusion. Since Al and Zr forms many intermediate compounds [11] one can assume that the interlayers consist of an amorphous Al-Zr alloy. The interlayers will contribute along with interface roughness to the total width of the interfaces [8], and result in reduction of the ML reflectance and grating efficiency because of blurring of the refractive index gradient.

Non-continuous diffraction rings are a clear sign of textural ordering in thin films. Indeed, the electron diffraction (Fig. 2, left) reveals strong axial texture for both materials with a $\langle 111 \rangle$ texture axis perpendicular to the substrate surface. Note, while the native bcc lattice was found for aluminum, Zr reflections correspond to a high-temperature (bcc) β -Zr phase rather than an equilibrium low-temperature (hexagonal) α -Zr phase. This issue requires some additional investigation in order to make sure, that high-temperature phase formation is not an artifact caused by the cross-sectional TEM sample preparation procedure.

Although high mobility of Al and Zr atoms suppresses the columnar growth regime and prevents multilayer stack perturbation observed earlier for a Mo/Si coating [12], too strong a

smoothing of the groove profile has a negative impact on the diffracting properties of the grating. Figure 3a shows a diffraction pattern obtained from the Al/Zr MBG at an incidence angle of 11° and a wavelength of 19.2 nm. There are three strong peaks which are the 1st, the 0th, and the -1st diffraction orders with efficiencies of 13.2%, 12.1%, and 10.8%, respectively. The diffraction efficiency of the blazed order is smaller than the Al/Zr witness reflectance of 49% almost by a factor of 4.

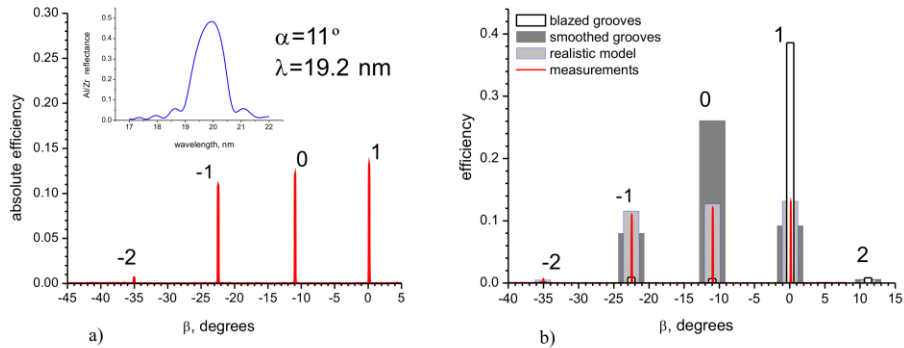


Fig. 3. Measurements (a) and simulations (b) of diffraction from the Al/Zr MBG for the incident angle of 11° and a wavelength of 19.2 nm. The insert shows the reflectance of the flat Al/Zr witness multilayer versus wavelength at the incidence angles of 5° . Simulations were performed for three models of a ML stack: a blazed model (open bars), a smoothed model (grey bars), and a realistic model (light grey bars).

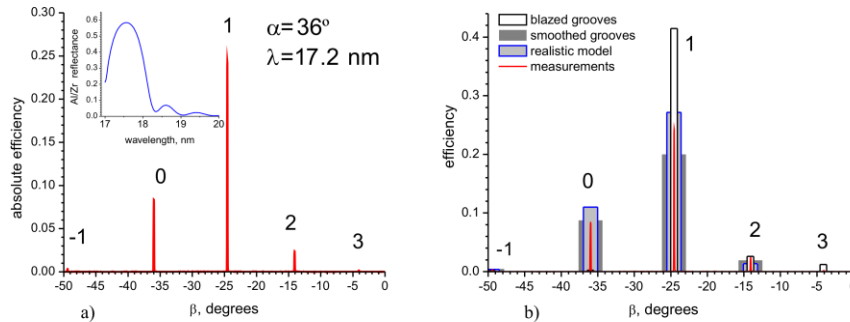


Fig. 4. The same as in Fig. 3, but for incidence angles of 36° and 30° for the grating and ML witness respectively.

Analysis of the diffraction data was performed by simulation of the diffraction efficiency for three different models of the multilayer stack. The blazed model assumed all the interfaces of the multilayer stack had the same sawtooth shape as the substrate (see solid curve in Fig. 1d). The smoothed model assumed a sine-like profile (see a dashed curve in Fig. 1d) for all the interfaces. The realistic model was composed using AFM and TEM data, and took into account the gradual transition from the blazed groove profile to the sine-like one through the ML stack. The average sawtooth substrate profile obtained with AFM measurements was used as the bottom interface of the model ML stack. The interface profile for each layer was obtained by Fourier smoothing of an underlying layer profile. The parameters of the smoothing were optimized in order to obtain a good match of the upper layer profile to the experimental one (dashed curve in Fig. 1d). The model assumed that all the smoothing was caused by the Al layers, while Zr layers replicated the underlying interfaces with no changes. Although this is an over-simplification of the real structure of the ML stack, it was found to not noticeably affect the results of the efficiency simulations.

The ML stack models used for simulation ignored the intermixing of materials mentioned above and interface roughness, and assumed perfect periodicity of the grating. In order to take into account interface imperfections and possible errors of the grating period all the calculated efficiency values were scaled by a factor of 0.74, which provided a good match of the simulated efficiency to the measured one.

The results of the efficiency simulations are shown in Fig. 3b. Comparison of the different models shows, that if the initial blazed groove profile of the substrate would have been preserved during the ML deposition, almost all diffraction energy would have been concentrated in the 1st blazed order, and diffraction efficiency would have reached 40%. On the other hand if all the interfaces had a sine-like shape of the top surface of the grating, the diffraction pattern would have had a strong zero order similar to holographic gratings. The simulation results obtained for the realistic model of the ML stack are in a good agreement with the experimental data. They show that the blazing ability of the grating weakened greatly due to the smoothing. Efficiency of the 1st blazed order is reduced by a factor of 3 as compared to the blazed grating. Nevertheless the grating still has some enhanced blazing as compared with a holographic one: the 1st order efficiency is higher by a factor of 1.4, and the zero order is significantly suppressed as against the one for the smoothed model.

For the angle of incidence of 36° the diffraction pattern consists of a strong 1st order blazed peak, and other orders are significantly suppressed (Fig. 4) at the wavelength of 17.2 nm. Efficiency of the grating rises up to 24.4%, which corresponds to a relative efficiency of 42% as compared to the reflectance of 57% of the Al/Zr witness multilayer (see an insertion in Fig. 4a). However the absolute efficiency is still smaller by a factor of 2.3 when compared to the one for the blazed model.

The observed concentration of diffracted energy in the 1st blazing order (Fig. 4) should be attributed to enhancement of blazing ability of holographic gratings at oblique illumination. Indeed, distribution of diffracted energy among the orders is quite similar for the realistic and smoothed models at the incidence angle of 36°. This is because of similarity of upper layers for both the models and the fact that contribution of the upper layers of the stack into the net ML reflectance increases with the incidence angle.

4. Summary

We successfully fabricated a high quality sawtooth substrate with a groove density of 10,000 lines/mm. The substrate coated with an Al/Zr multilayer EUV reflector demonstrated an absolute efficiency in the 1st diffraction order as high as 13% and 24% at the incident angles of 11° and 36° respectively.

The high smoothing ability of the multilayer suppresses undesirable shadowing effects and provides deposition of continuous layers of the coating on the highly corrugated surface of the substrate. However the Al/Zr multilayer smoothes the sawtooth profile of the grating grooves too much, and results in substantial degradation of the blaze performance of the MBG.

This study shows that deposition of multilayers on sawtooth substrates is currently the biggest challenge for development of ultra-dense blazed MBGs. The ideal deposition process should avoid shadowing effects, provide effective relaxation of high-frequency random thickness variations, and at the same time provide conformal replication of the sawtooth profile by the coating. Addressing this problem requires precise tuning of the smoothing ability of a multilayer by optimal choice of multilayer materials, deposition geometry and deposition parameters. A possible way of doing this is collimation of the atomic flux to minimize shadowing, and optimization of the energy of arriving atoms in order to control their surface mobility. Optimization of these parameters is the subject of our current work.

Acknowledgments

This work was supported by the U. S. Department of Energy under contract number DE-AC02-05CH11231.